Heliyon 10 (2024) e23582

Contents lists available at ScienceDirect

Heliyon

journal homepage: www.cell.com/heliyon

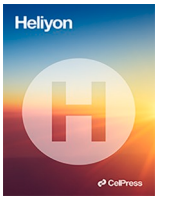

In silico analyses of pan-squamous cell carcinoma unveiled the immunological implications of MRPL13, which had previously been under-recognized

Yan Liang [a], Shuo He [a], Yiyi Tan [b], Qing Liu [b], Feng Zhao [b], Tao Liu [c], Conggai Huang [d], Xiaomei Lu [b,**], Shutao Zheng [b,*]

[a] Department of Pathology, Basic Medicine College, Xinjiang Medical University, Urumqi, 830017, China
[b] State Key Laboratory of Pathogenesis, Prevention, Treatment of Central Asian High Incidence Diseases, Clinical Medical Research Institute, First Affiliated Hospital of Xinjiang Medical University, Xinjiang Uygur Autonomous Region, Urumqi, China
[c] Department of Clinical Laboratory, First Affiliated Hospital of Xinjiang Medical University, Xinjiang Uygur Autonomous Region, Urumqi, China
[d] Department of Pathology, The Affiliated Hospital of Southwest Medical University, Luzhou, 646000, China

ARTICLE INFO

Keywords:
MRPL13
Pan-squamous cell carcinoma
Bioinformatics analysis
Prognostic
$CD8^+$ T-cell infiltration

ABSTRACT

The involvement of the mitochondrial ribosomal protein 13 (MRPL13) gene in the development of adenocarcinoma has been previously reported. However, the clinicopathological significance of MRPL13 in squamous cell carcinoma (SCC) remains poorly understood. To gain insight into the clinicopathological and immunological implications of MRPL13 expression in SCC, we conducted a bioinformatic analysis utilizing various available databases, including TIMER 2.0, Xiantao academic tool and TISIDB, attempting to evaluate the abnormal expression, prognosis and immunological correlation of MRPL13 in the pan-SCC setting. Subsequently, we conducted experimental verification using an esophageal squamous cell carcinoma (ESCC) tissue array subjected to multiplexed immunofluorescent (mIF) staining. The ESCC tissue array we used consists of 93 dots of ESCC and 86 dots of matched adjacent normal tissues (ANT). Data from in silico analyses showed that MRPL13 mRNA is significantly up-regulated and correlated with infiltration of $CD8^+$ T cells in pan-SCC. However, in silico analyses did not support the prognostic role of MRPL13 in SCC. Consistently, data from the ESCC tissue array showed that MRPL13 was remarkably elevated in ESCC tissues relative to ANT in stroma, which was controlled by pan-cytokeratin (pan-CK) staining. In the epithelia, no significant difference was identified between ESCC and ANT. Furthermore, MRPL13 expression markedly correlated with the infiltration of $CD8^+$ T cells in the stromal region but not in the epithelial region. Prognostically, no significant association was observed between MRPL13 expression and overall survival, regardless of epithelial or stromal section. Through these pan-SCC analyses, we have expanded the understanding of MRPL13 previously reported, in particular, underscoring the immunological involvement of MRPL13 in the tumor microenvironment of SCC that has been under-recognized before, suggesting that MRPL13 may regulate the infiltration of $CD8^+$ T cells into the SCC microenvironment.

* Corresponding author.
** Corresponding author.
E-mail addresses: luxiaomei@xjmu.edu.cn (X. Lu), zhengshutao@xjmu.edu.cn (S. Zheng).

https://doi.org/10.1016/j.heliyon.2023.e23582
Received 12 June 2023; Received in revised form 6 December 2023; Accepted 7 December 2023
Available online 14 December 2023

1. Introduction

Mitochondrial ribosomal protein L13, shortened for MRPL13, a member of the MRP family, is located on chromosome 8q24.12 and belongs to the primary binding protein that combines with rRNA to form mitochondrial ribosomes and participates in the biosynthesis

Abbreviations

CESC	Cervical squamous cell carcinoma and endocervical adenocarcinoma
ESCA	Esophageal carcinoma
HNSC	Head and Neck squamous cell carcinoma
LUSC	Lung squamous cell carcinoma

of mitochondrial proteins [1]. Mitochondria are key organelles that play a pivotal role in regulating the energy of eukaryotic cells and participate in the internal pathway regulating cell apoptosis [2,3]. Inducing the apoptosis and proliferation of cancer cells through mitochondrial translation and mitotic ribosomal proteins, MRPs are closely related to the prognosis and development of tumors. A good supporting example from a recent study revealed that the expression of MRPL13 in breast adenocarcinoma was significantly higher than that in adjacent tissue, which may indicate a poor prognosis of breast adenocarcinoma [4]. Another example supporting the important role of MRPL13 comes from liver cancer [5], where inhibiting the expression of MRPL13 is the key to oxidative phosphorylation dysfunction, which leads to enhancement of the invasion of liver cancer cells. Despite these sporadic reports regarding MRPL13, little is known concerning the involvement of MRPL13 in the setting of squamous cell carcinoma (SCC).

In total, unlike adenocarcinoma, SCC is an epithelial malignancy that occurs in organs normally covered with squamous epithelium that includes the mouth, esophagus, lungs, cervix and so forth. The majority of SCC cases, therefore, were from head and neck cancer, esophageal cancer and lung cancer. Strongly associated with a high risk of recurrence and metastasis, SCC results in significant mortality and thus requires personalized treatment [6–8]. In light of the distinctively different landscape of the immune microenvironment between adenocarcinoma and SCC, for instance, lung cancer [9], it makes much sense that patients with different subtypes of lung cancer will have different clinical outcomes even when treated with immune checkpoint blockades [10]. Compelling evidence supporting this notion came from a comparative study between lung adenocarcinoma and SCC [10], revealing that tumor mutation burden level, programmed cell death ligand 1 (PD-L1) expression, and tumor infiltrating lymphocytes (TILs) in the tumor microenvironment within the two subtypes may lead to different responses to immune checkpoint blockade therapy. It has been revealed that the infiltrating density of $CD8^+$ TILs is a poor prognostic factor in lung adenocarcinoma but a favorable prognostic factor in SCC of the lung [11]. Hence, understanding the regulation of infiltration of $CD8^+$ T cells will be pivotal for improving treatment in SCC.

Collating the literature regarding the investigation performed on regulation of infiltration of $CD8^+$ T cells into tumors, several possible mechanisms can be easily summarized into the following two aspects: activation of signaling pathways [12,13] and abnormalities in genes, including PAK4 [14,15] and PTEN [16]. Beyond these previously reported findings, we, by using in silico analyses of cancer databases, preliminarily found that MRPL13 could also be involved in the modulation of infiltration of $CD8^+$ T cells into SCC. To date, no investigation has been performed on the oncoimmunological implication of MRPL13 in SCC. Given this, we selected MRPL13 as a gene of interest to better understand its immunological involvement in the pan-SCC context through deliberate analyses based on the available bioinformatic databases plus experimental confirmation using an ESCC tissue array. This is the first report investigating the immunological involvement of MRPL13 expression in SCC.

2. Materials and methods

2.1. Gene expression analysis of MRPL13

The "Gene DE" module of tumor immune evaluation resource version 2.0 (TIMER 2.0) [17] (http://timer.cistrome.org/) was used to investigate the difference in MRPL13 expression between tumor and non-tumor tissues of various tumor types. The gene expression levels are represented as log 2 TPM values. Moreover, databases such as the Xiantao academic platform [18] (https://www.xiantao.love/) were also consulted when appraising MRPL13 differential expression between tumors and matched normal controls. Student's *t*-test was used to evaluate the significance of the difference, and $P < 0.05$ was considered statistically significant.

2.2. Prognostic analyses of MRPL13

Overall survival OS Kaplan–Meier plots of MRPL13 in all TCGA tumor types were generated using the Gene Expression Profiling Interactive Analysis version 2 (GEPIA2) [19] (http://gepia2.cancer-pku.cn/) "Survival Analysis" module and "lymphocyte" module of an integrated repository portal for tumor-immune system interactions (TISIDB) [20] (http://cis.hku.hk/TISIDB/). The expression threshold was set at 50 % for high MRPL13 expression and low MRPL13 expression.

2.3. Immune cell infiltration analysis of MRPL13

For reliable evaluation of immune infiltration and immune checkpoint-related genes, we consulted with the "lymphocyte" module of an integrated repository portal for tumor-immune system interactions (TISIDB) [20] (http://cis.hku.hk/TISIDB/). A Spearman correlation analysis scatter map was used to analyze the potential correlation between the expression of immune checkpoint-related genes and MRPL13 genes in Pan-SCC.

2.4. Tissue array of ESCC

The ESCC tissue array was outsourced to Shanghai Outdo Biotech. Co. Ltd. (Superchip, Shanghai, China). The tissue array we used consisted of 93 cases of ESCC and 87 cases of matched adjacent normal control (ANT) tissues. The clinicopathological parameters comprising demographics, clinical stage, TNM classifications, and overall survival were documented when available. Noticeably, among these 93 cases of ESCC, seven cases had unavailable follow-up data, which means that only 86 cases had follow-up data. Moreover, only 82 cases had information related to invasion degree, with 11 cases being unavailable, and 91 cases had gross morphology, with two cases missing the information. Staging and grading of the ESCC tissues used to produce the tissue array were determined depending on hematoxylin and eosin (H&E) staining. Histopathological diagnoses of ESCC tissues were based on the criteria of the World Health Organization 2017 version. None of the samples were gleaned from patients undergoing chemoradiotherapy before esophagectomy. The study was approved by the medical ethics committee of the First Affiliated Hospital of Xinjiang Medical University. Written informed consent was obtained from each participant involved.

2.5. Multiplexed immunofluorescent (mIF) staining

As previously described [21,22], in brief, samples were cut into 5 μm thick sections and loaded onto adhesion microscope slides. The slides were preprocessed with deparaffinization, rehydration, and antigen retrieval for mIF staining. Multiplexed immunofluorescence staining of tissue was performed using TG TSA Multiplex IHC Assay Kits (TissueGnostics Asia-Pacific Ltd.) primary antibody against pan-CK (catalog number: ab7753, Abcam; dilution at 1:4000), CD8A (catalog number: ABS171634, Absin Inc.; dilution at

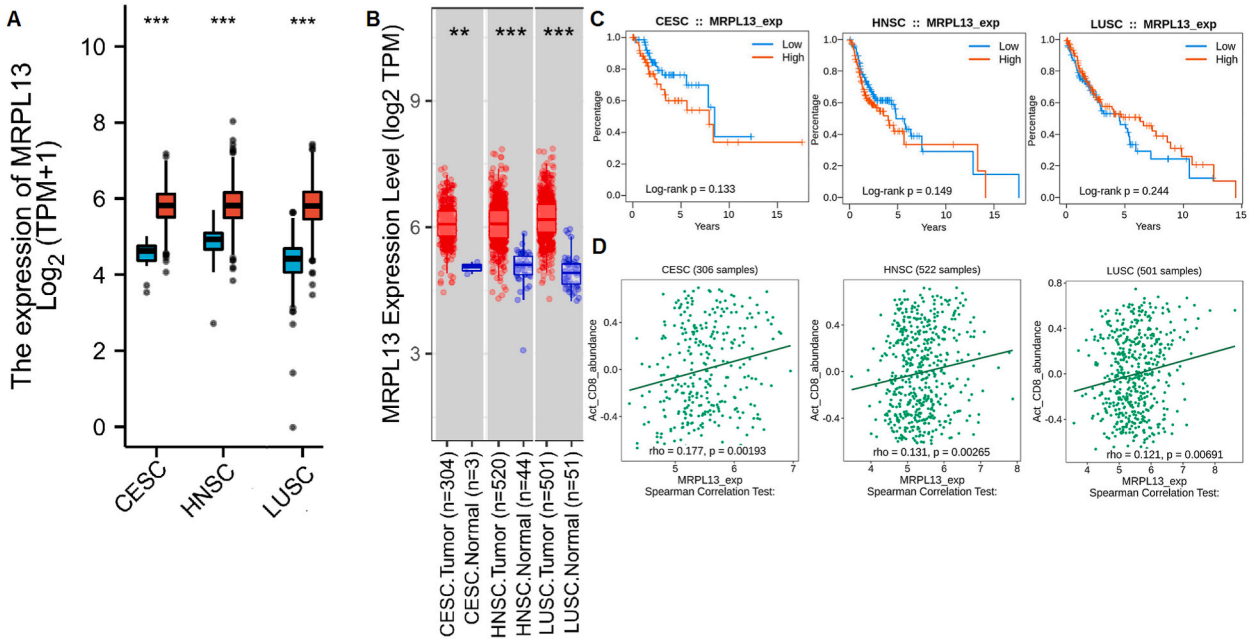

Fig. 1. Pan-squamous cell carcinoma analyses showing the implications of MRPL13 expression in overall survival and correlation with infiltration of $CD8^+$ T cells into cervical squamous cell carcinoma (CSCC), head and neck squamous cell carcinoma (HNSCC) and lung squamous cell carcinoma (LUSC). **A**: Higher expression of MRPL13 was analyzed in CSCC, HNSCC and LUSC retrieved from the TCGA and GTEx databases using the Xiantao academic platform tool (https://www.xiantao.love/). The image was available from and credited to the Xiantao academic platform; **B:** Likewise, confirmation of MRPL13 expression status in CSCC, HNSCC and LUSC was analyzed by the TIMER 2.0 database (http://timer.cistrome.org/). Asterisks, such as ** or *** indicate that MRPL13 expression was significantly increased in cancer tissues. The image was from and credited to the TIMER 2.0 database. **C**: Prognostic evaluation of MRPL13 expression in CSCC, HNSCC and LUSC was performed using the TISIDB database (http://cis.hku.hk/TISIDB/). The Kaplan–Meier plots presented were directly from and credited to the TISIDB database. **D**: The correlation between MRPL13 expression and the infiltrating intensity of activated $CD8^+$ T cells was also analyzed by the TISIDB database (http://cis.hku.hk/TISIDB/). The correlational plots shown were credited to the TISIDB database.

1:1000), MRPL13 (catalog number: ABS140737, Absin Inc.; dilution at 1:200), second antibody (catalog number: PV-6002 and PV-6001; Zhongshan Goldbridge Biotechnology, China; ready-to-use), and NEON E-TSA Smart 540 seven-color kit from HISTOVA company (Beijing histova Biotechnology Co., Ltd). The cell density nucleus area per cell and expression per cell were quantified using StrataQuest software (version 7.1.119, TissueGnostics GmbH, Vienna, Austria). Visualization of the different fluorophores was achieved on the TissueFAXS Spectra Systems (TissueGnostics GmbH, Vienna Austria) and StrataQuest analysis software (Version 7.1.129, TissueGnostics GmbH, Vienna, Austria).

2.6. Statistical analyses

The chi-square test was used to compare clinicopathological characteristics between the high and low MRPL13 subgroups. Notably, when the expected number was less than 5, Fisher's exact test was applied. For survival, the start date was the beginning of treatment, ending with the last follow-up date or death. The Mann–Whitney *U* test was employed to assess the difference in the expression of MRPL13 between ESCC and ANT after checking the data that did not conform to the normal distribution. Similarly, Spearman correlation analyses were used to analyze the correlation between the number of $CD8^+$ T cells and the number of MRPL13 cells after determination of data that did not follow the normal distribution. Kaplan–Meier survival curves were plotted to assess the overall survival of MRPL13 expression; log-rank tests were used to calculate the survival difference. A P value of <0.05 was considered statistically significant. Statistical analyses were carried out using SPSS version 17.0 (SPSS, Chicago, USA), and GraphPad Prism 8.0

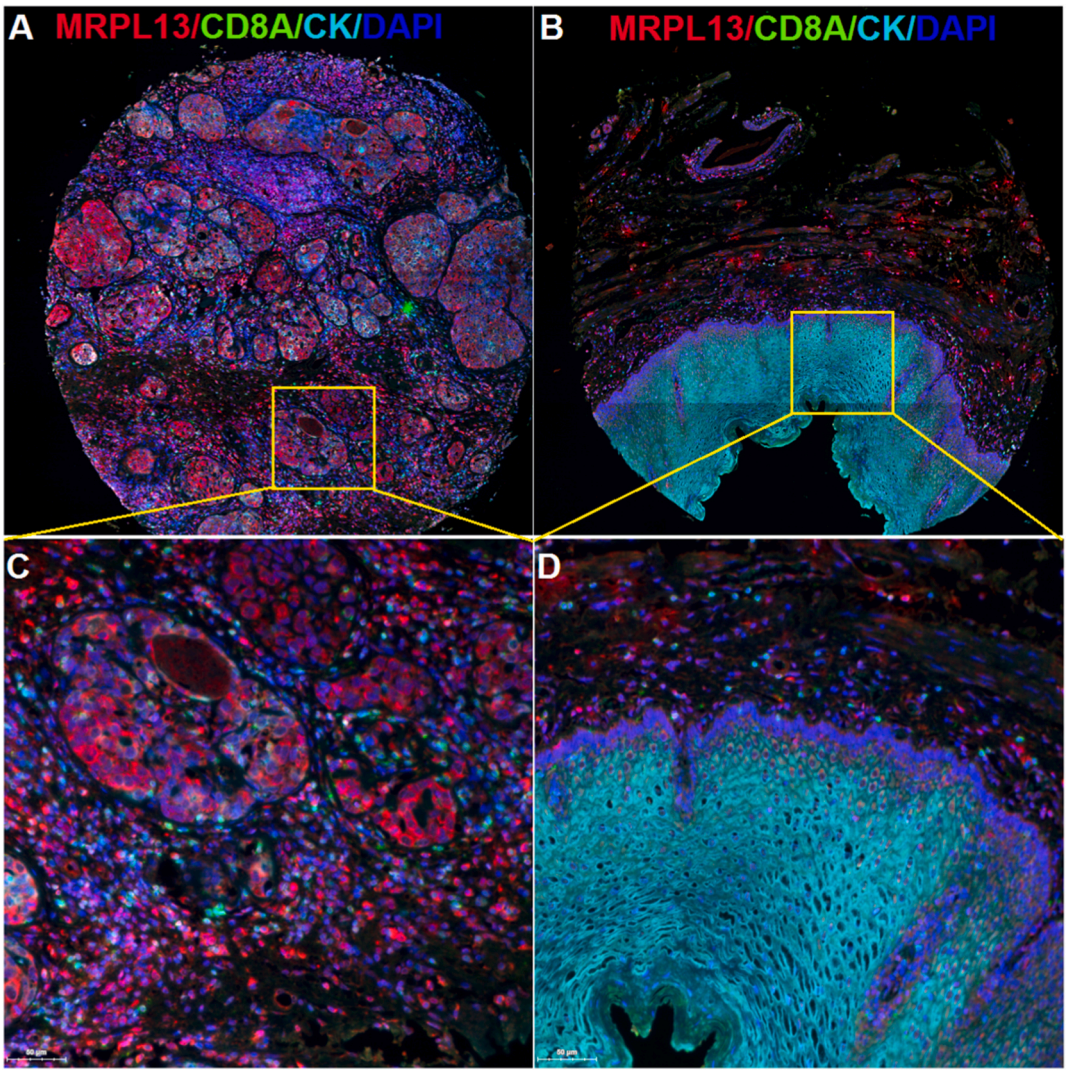

Fig. 2. Multiplexed immunofluorescence (mIF) staining images showing the expression of MRPL13, CD8A, Pan-cytokeratin (Pan-CK) and DAPI in paired esophageal squamous cell carcinoma (ESCC) and matched adjacent normal tissue (ANT) controls. **A:** ESCC tissue displaying the expression of MRPL13, CD8A, Pan-CK and DAPI; **B:** ANT tissue on which MRPL13, CD8A, Pan-CK and DAPI were immunostained; **C:** magnification of inset of ESCC; **D:** similarly, magnification of inset area of ANT. Scale bar, 50 μm. Pan-CK served as a biomarker differentiating epithelia from stroma.

(San Diego, CA, USA) was used to plot the histograms.

3. Results

3.1. In silico analyses of implications of MRPL13 expression in a pan-squamous cell carcinoma setting

First, to understand the involvement of MRPL13 expression in the setting of squamous cell carcinoma (SCC), we tried to address this problem by resorting to an in silico analysis approach. Taking advantage of databases that have been open, free and ready to use for investigators, such as the Xiantao academic platform designed and made by Chinese researchers, we found that MRPL13 was significantly elevated in cancerous tissues compared with normal controls, irrespective of the type we were concerned with, including cervical squamous cell carcinoma (CSCC), head and neck squamous cell carcinoma (HNSCC) and lung squamous cell carcinoma (LUSC) (Fig. 1A). To verify the expression trend we observed using the Xiantao academic on line tool, we employed another convenient database for users: the TIMER 2.0 database. Consistent with data from the Xiantao academic platform, data from the TIMER 2.0 database showed that MRPL13 was markedly up-regulated in cancerous tissues relative to normal controls at the mRNA level (Fig. 1B). Next, to understand the prognostic meaning of MRPL13 expression in Pan-SCC, including CSCC, HNSCC and LUSC, we used the TIMER 2.0 database to analyze the prognosis of MRPL13, showing that no significant association was identified between overall survival and MRPL13 expression at the mRNA level (Fig. 1C). Meanwhile, we used another database, GEPIA 2.0, to confirm what we observed in regard to the prognosis of MRPL13 expression. In agreement with the prognosis analyzed from TIMER 2.0, prognostic analyses from the GEPIA 2.0 database also supported the prognostic meaninglessness of MRPL13 expression (Supplementary Fig. 1). Next, we explored the correlation between MRPL13 expression at the mRNA level and infiltration of $CD8^+$ T cells in the Pan-SCC setting, observing that MRPL13 expression was remarkably correlated with the infiltration of $CD8^+$ T cells in cancerous tissues, regardless of the type of SCC (Fig. 1D). Taken together, these data explicitly indicated the heavy implication of MRPL13 expression at the mRNA level in the immune infiltration of SCC.

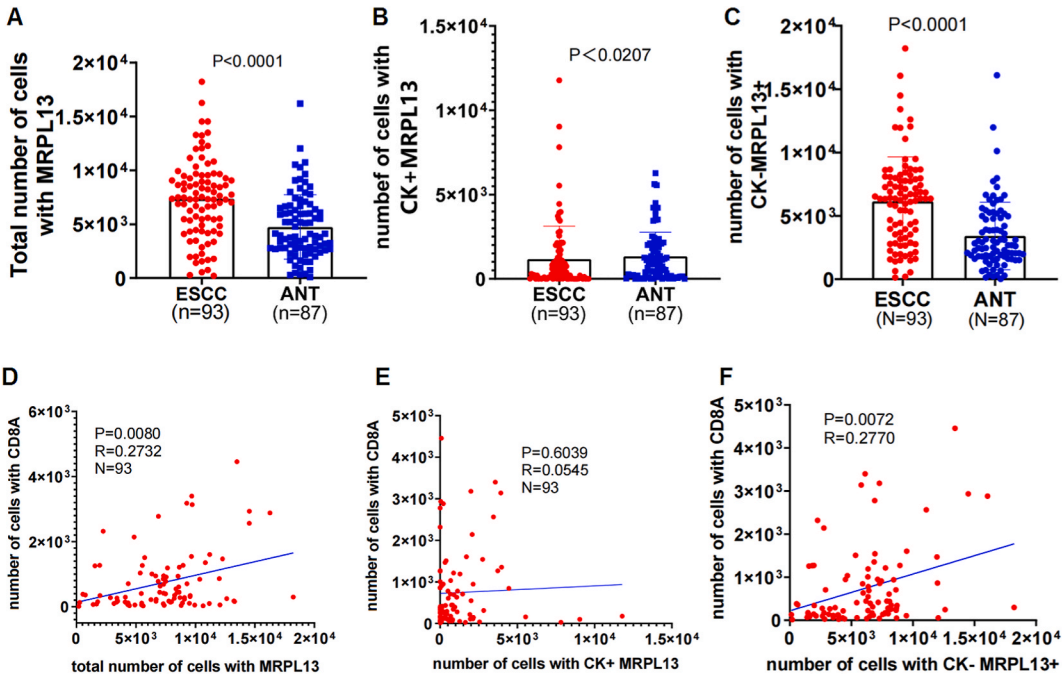

Fig. 3. The implications of MRPL13 expression in overall survival and infiltration of $CD8^+$ T cells into ESCC tissues were statistically analyzed. A: The significant difference in the total number of cells stained with positive MRPL13 expression between ESCC and ANT tissues. **B:** Likewise, there was a significant difference in the number of cells stained with positive Pan-CK (CK+) and MRPL13 expression between ESCC and ANT tissues. **C:** The difference in the number of cells stained with negative Pan-CK (CK-) and positive MRPL13 (MRPL13 +) expression between ESCC and ANT tissues is presented. In histograms from A through C, two-tailed Mann−Whitney U tests were employed. **D:** The correlation between the number of cells with CD8A and the total number of cells with MRPL13 in ESCC tissues, totaling 93 cases. **E:** Correlational analysis between the number of cells with CD8A and the total number of cells with positive Pan-CK and positive MRPL13 in ESCC tissues; **F:** correlation between the number of cells with CD8A and the total number of cells with negative Pan-CK and positive MRPL13 in ESCC tissues, totaling 93 cases. In the correlation plots shown from D through F, the Spearman correlation analysis method was used.

3.2. MRPL13 expression in esophageal squamous cell carcinoma (ESCC)

Having understood the immunological implication of MRPL13 in the Pan-SCC setting, we subsequently confirmed all that was observed using in silico analyses in ESCC tissues collected on our own. Thanks to the multiplexed immunofluorescent (mIF) staining technique that has been well received and applied since its advent, we were able to evaluate the expression of MRPL13 and infiltrating intensities of $CD8^+$ T cells in ESCC (Supplementary Fig. 2). As its name suggests, SCC originates from squamous epithelia that can be identified by immunostaining with cytokeratin. Here, pan-cytokeratin (hereafter short for CK) was used as a tumor biomarker controlling its origination from epithelia instead of stromal cells (Fig. 2). DAPI nuclear staining was used to quantify cell numbers. Taken as a whole, the total number of cells stained with MRPL13 was shown to be dramatically up-regulated in ESCC tissues in comparison with ANT (Fig. 3A), which was in agreement with data from in silico analyses (Fig. 1A and B). Specifically, for tumor cells from the epithelial region where the tumor cells were CK-negative and MRPL13-positive, compared with ANT, MRPL13 was pronouncedly reduced in ESCC tissues (Fig. 3B). In contrast to tumor cells from epithelia, MRPL13 was drastically elevated in ESCC cells relative to ANT from the stromal region, in which tumor cells were double positive for CK and MRPL13 (Fig. 3C). Clinicopathologically, when analyzed overall, irrespective of the epithelial or stromal region, only tumor grade was significantly correlated with MRPL13 expression (Table 1). No other significant correlation was observed between MRPL13 expression and other clinicopathological parameters, such as gender, age, tumor size, gross morph and invasion degree (Table 1). In the stromal region, in addition to a significant correlation with tumor grade, MRPL13 expression was also observed to be markedly correlated with invasion degree (Table 1). However, no significant correlation was identified in the epithelial region, which was denoted by double-positive staining with CK and MRPL13.

3.3. Immunological and prognostic involvement of MRPL13 expression in ESCC

Next, we analyzed the immunological implication of MRPL13 expression in ESCC, showing that without respect to tumor cells from the epithelial or stromal region, there was a significant correlation between the total number of cells stained with MRPL13 and the number of $CD8^+$ T cells (Fig. 3D). For tumor cells from the stromal region where tumor cells were CK-negative and MRPL13-positive, no significant correlation was found between the number of cells negative for CK but positive for MRPL13 and the number of $CD8^+$ T

Table 1
Clinicopathological significance of MRPL13 expression in ESCC.

Parameters		Total MRPL13		χ^2	*P*	CK + MRPL13+		χ^2	*P*	CK-MRPL13+		χ^2	*P*
		High	Low			High	Low			High	Low		
Gender	male	47	30	0.127	0.783	29	48	3.774	0.079	47	30	0.127	0.783
	female	9	7			2	14			9	7		
Age (years)	≤60	14	13	1.111	0.353	12	15	2.114	0.225	14	13	1.111	0.353
	> 60	42	24			19	47			42	24		
tumor size (cm)	< 3	4	4	0.381	0.709	2	6	0.274	0.714	4	4	0.381	0.709
	≥3	52	33			29	56			52	33		
Grade	I	5	9	11.708	**0.021**	4	10	3.082	0.698	6	8	11.026	**0.031**
	II	15	15			9	21			14	16		
	III	5	0			1	4			5	0		
	I-II	22	8			12	18			22	8		
	I-III	0	1			1	0			0	1		
	II-III	9	4			4	9			9	4		
Morphology	medullary	14	10	4.505	0.308	8	16	2.468	0.687	13	11	4.023	0.364
	plaque	0	2			1	1			0	2		
	ulcer	32	18			19	31			32	18		
	fungi	6	2			1	7			6	2		
	protrude	3	4			2	5			4	3		
Invasion	muscularis	13	6	4.576	0.205	5	14	0.979	0.925	13	6	5.426	0.116
	submucosa	0	3			1	2			0	3		
	adventitia	34	25			20	39			33	26		
	full layer	3	2			2	3			4	1		
Location	upper	41	29	1.122	0.835	23	47	1.034	0.823	41	29	1.122	0.835
	middle	8	5			5	8			8	5		
	lower	6	2			3	5			6	2		
	middle-lower	1	1			0	2			1	1		
T classification	T1	0	3	4.791	0.154	1	2	3.938	0.210	0	3	4.791	0.154
	T2	13	6			5	14			13	6		
	T3	36	26			20	42			36	26		
	T4	1	1			2	0			1	1		
N classification	N0	24	21	5.092	0.149	16	29	0.492	0.949	25	20	4.265	0.216
	N1	18	9			8	19			17	10		
	N2	13	4			6	11			13	4		
	N3	1	3			1	3			1	3		

cells (Fig. 3E). For tumor cells from epithelia, a marked correlation was identified between the number of cells double positive for CK and MRPL13 and the number of $CD8^+$ T cells (Fig. 3F). Furthermore, we undertook prognostic analyses regarding MRPL13 expression in ESCC. MRPL13 expression was unassociated with overall survival, regardless of epithelial, stromal or ESCC status (Fig. 4A to C). We also analyzed the distributional difference of $CD8^+$ T cells between ESCC and ANT tissues, revealing that no significant difference can be found between ESCC and ANT (Supplementary Fig. 3A). Moreover, the infiltration intensity of $CD8^+$ T cells was not associated with the overall survival of ESCC tissues (Supplementary Fig. 3B). Intriguingly, a remarkable correlation was identified between the infiltration intensity of $CD8^+$ T cells and the gross morphology of ESCC (Supplementary Table 1). Collectively, the data we obtained from this section indicated that MRPL13 expression could be heavily implicated in the regulation of infiltration of $CD8^+$ T cells but unrelated to prognosis in ESCC tissues.

4. Discussion

In this investigation, drawing on in silico analyses of data regarding squamous cell carcinoma explicitly included in the TCGA database, we found that MRPL13 was markedly elevated at the mRNA level in all SCC types included in the TCGA database. Prognostic analyses of data from the available database revealed that elevated MRPL13 was unrelated to overall survival in SCC. However, we discovered that MRPL13 has important immunological involvement in the tumor microenvironment of SCC, which has been unrecognized ever before, based on pan-SCC analyses. As a verification of the immunological implication of MRPL13 suggested by bioinformatic analyses in SCC, we confirmed it using an ESCC tissue array of our own by means of mIF staining approach. The data from ESCC completely supported what was observed by bioinformatic analyses. Our study described here was important in that our analyses expanded the current understanding of MRPL13 in the tumor setting.

MRPL13, abbreviated for mitochondrial ribosomal protein L13, is also known as L13mt, RPML13, RPL13 or L13, which is far less commonly used than MRPL13. As its name suggests, MRPL13 is a kind of protein that is related to mitochondrial ribosomes [23] that are bound to consist of large and small subunits. Few studies have deliberately investigated the possible biological or clinical involvement of MRPL13 in the setting of cancer. In contrast, several lines of evidence from basic research revealed that MRPL13 was critical for the structural and functional integrity of the mitochondria [1] and engaged in the organization of the tunnel exit of mitochondria [24]. In addition, little is known regarding the biochemical or physiological function of MRPL13. Therefore, we undertook a comprehensive approach grounded in bioinformatic analyses to explore the possible biological roles of MRPL13 in the biological process of cells (data not shown). Gene Ontology (GO) annotations suggested the novel roles of MRPL13, including RNA binding and structural constituents of ribosomes, which need to be further investigated based on experimental design. Through the KEGG database, we found that MRPL13 actively participated in several pathways. It should be stressed here that among its related pathways are mitochondrial translation and metabolism of proteins. Of course, all the suggestions given by GO and KEGG analyses described here require further confirmation by experiments.

Until recently, there seems to be a resurgence of studies regarding MRPL13 in cancer, indicating that MRPL13 could strongly drive the proliferation and motility of cancer cells *in vitro* [2,4] regardless of cancer type. Apart from experiments conducted *in vitro* in cell culture, several lines of evidence from recent studies involving clinical tissues explicitly suggested the prognostic prediction value of MRPL13 in the context of adenocarcinoma, which is histopathologically different from squamous cell carcinoma. Several supporting examples were from breast adenocarcinoma [25–28]. Among these four studies reviewed above, there was high agreement with one another on the point that MRPL13 expression was closely associated with the overall survival of patients with breast adenocarcinoma. Consistently, this notion was also supported by several investigations based on total and purely bioinformatic analyses in breast adenocarcinoma [29–31]. Nevertheless, this is not the case at all in the setting of squamous cell carcinoma. In our analysis, in stark contrast with breast adenocarcinoma, the expression of MRPL13 was totally unrelated to the overall survival of squamous cell carcinoma.

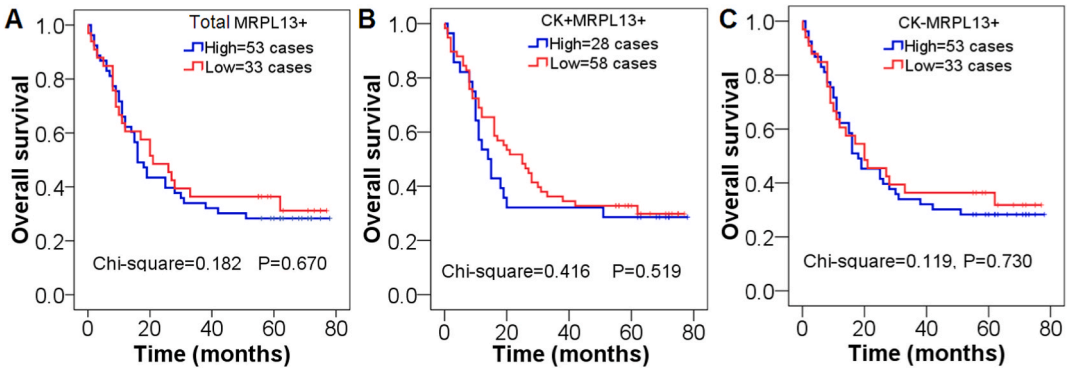

Fig. 4. The prognostic significance of MRPL13 expression in ESCC is presented. **A**: overall survival of ESCC tissues with high and low total number of cells stained with MRPL13; **B:** in the same manner, overall survival difference between ESCC tissues with high and low CK + MRPL13+ cells; **C:** likewise, overall survival difference between ESCC tissues with high and low CK- MRPL13+ cells. Kaplan–Meier survival curves were plotted; log-rank tests were used from plots A through C.

As stated in the preceding paragraph, before our study, there were several articles published already mainly in the adenocarcinoma context, which were performed totally based on pure bioinformatic analyses [29] [27,30,31], consistently reporting that MRPL13 was significantly associated with overall prognosis in breast adenocarcinoma. In particular, the findings contributed by Lin X et al. [29] should be mentioned here that the authors systemically analyzed the expression and prognostic significance of the mitochondrial ribosomal protein (MRP) family, including MRPL1, MRPL13, MRPS6, MRPL16, MRPS18C and MRPS35, in breast adenocarcinoma. However, the immunological involvement of MRPL13 seems to have been overlooked in their deliberate investigation. In contrast, no study has emerged to date exploring the clinicopathological implication of MRPL13 expression in the setting of squamous cell carcinoma. Therefore, our study was not simply a patchwork for these previous studies but first explored the immunological involvement of MRPL13 in the setting of squamous cell carcinoma that has been previously unrecognized. In our study, we showed that the expression of MRPL13 significantly correlated with the infiltration of $CD8^+$ T cells in squamous cell carcinoma, which has never been reported before. In terms of the clinical significance of MRPL13 expression in squamous cell carcinoma, the up-regulation of MRPL13 was shown to be significantly related to tumor grade. As of this writing, the clinicopathological significance of MRPL13 expression in the SCC context remains less well known and thus requires further confirmation with a larger sample size in SCC types other than ESCC.

Aside from breast adenocarcinoma and non-small cell lung adenocarcinoma [2], where MRPL13 has been superficially investigated, the biological roles and pathological meaning of MRPL13 have been largely underreported in other types of cancer, let alone in squamous cell carcinoma. We therefore systematically analyzed MRPL13 across squamous cell carcinomas explicitly included in TCGA, including CSCC, HNSCC and LUSC. It should be noted that we did not think of ESCA (esophageal carcinoma) from the outset in that data related to ESCA included in TCGA were actually conflated with a small part of squamous cell carcinoma and the bulk of adenocarcinoma of esophagus, which could contaminate our Pan-SCC analyses. The same also holds true of CSCC included in TCGA, which strictly speaking was composed of the majority of cases concerning cervical squamous cell carcinoma and the minority of cases regarding endocervical adenocarcinoma. Therefore, it is not surprising that sometimes there was a certain disagreement between analyses from HNSCC or LUSC and CSCC that was not pure SCC in terms of component. As a good example, we also explored the relationship between MRPL13 expression and common immune checkpoint molecules other than $CD8^+$ T cells. It is worth noting that the immunosuppressive molecules PD-L1 (CD274) and TIGIT were significantly and negatively correlated with the expression of MRPL13 only in HNSCC and LUSC but not in CSCC (Supplementary Fig. 4).

There were also limitations that should have been recognized in this study. First, our study only analyzed the correlation of MRPL13 expression with the infiltration of $CD8^+$ T cells in ESCC. Subsequent and substantial experiments will be needed to further determine the possible mechanism of MRPL13 in ESCC. Second, the sample size of ESCC patients we employed was relatively small, which may lead to insufficient statistical power when interpreting the data.

5. Conclusion

In conclusion, our study underscores the novel immunological involvement of MRPL13 that has been previously under-recognized. Our original findings gleaned from in silico analyses plus mIF staining confirmation on ESCC will undoubtedly enrich our current understanding of MRPL13 in the setting of squamous cell carcinoma.

Funding

The study was partly supported by special funds for the development of local science and technology from the central government (ZYYD2022B06), grants from the Xinjiang Science Fund for Distinguished Young Scholars (2022D01E26), the Natural Science Foundation of China (Grant Nos. 81,960,552, 81,960,527), and partly by State Key Laboratory of Pathogenesis, Prevention and Treatment of High Incidence Diseases in Central Asia Fund (SKL-HIDCA-2020-SG1 ， SKL-HIDCA-2021-26).

Data availability

All data generated or analyzed during this study are included in this published article, along with supplementary information files. Data will be made available on request from corresponding author.

Consent for publication

Not applicable.

CRediT authorship contribution statement

Yan Liang: Writing – original draft, Data curation. **Shuo He:** Writing – original draft, Formal analysis. **Yiyi Tan:** Writing – original draft. **Qing Liu:** Writing – review & editing. **Tao Liu:** Writing – review & editing. **Conggai Huang:** Writing – review & editing. **Feng Zhao:** Writing - review & editing. **Xiaomei Lu:** Writing – review & editing, Supervision. **Shutao Zheng:** Writing – review & editing, Supervision, Conceptualization.

Declaration of competing interest

The authors declare the following financial interests/personal relationships which may be considered as potential competing interests: Shutao Zheng reports was provided by State Key Laboratory of Pathogenesis, Prevention and Treatment of High Incidence Diseases in Central Asia, Clinical Medical Research Institute, The First Affiliated Hospital of Xinjiang Medical University, Urumqi 830,054, Xinjiang, PR China. Shutao Zheng reports a relationship with State Key Laboratory of Pathogenesis, Prevention and Treatment of High Incidence Diseases in Central Asia, Clinical Medical Research Institute, The First Affiliated Hospital of Xinjiang Medical University, Urumqi 830,054, Xinjiang, PR China that includes: funding grants.

Acknowledgment

Special thanks go to the Xiantao academic platform, GEPIA 2.0 and TIMER 2.0 databases we have been exploiting throughout the study. We also thank TissueGnostics Aisa Pacific limited (Beijing, China) for their excellent technical support for multiplexed immunofluorescence staining, image scanning and analysis and the help of Enjia Li, the experienced technician and Andrew Guo, the data engineer.

Appendix A. Supplementary data

Supplementary data to this article can be found online at https://doi.org/10.1016/j.heliyon.2023.e23582.

References

[1] H. Ke, S. Dass, J.M. Morrisey, M.W. Mather, A.B. Vaidya, The mitochondrial ribosomal protein L13 is critical for the structural and functional integrity of the mitochondrion in Plasmodium falciparum, J. Biol. Chem. 293 (21) (2018) 8128–8137, https://doi.org/10.1074/jbc.RA118.002552.
[2] C. Jing, R. Fu, C. Wang, X. Li, W. Zhang, MRPL13 act as a novel therapeutic target and could promote cell proliferation in non-small cell lung cancer, Cancer Manag. Res. 13 (2021) 5535–5545, https://doi.org/10.2147/CMAR.S316428.
[3] E. Klæstad, S. Opdahl, M.J. Engstrøm, et al., MRPS23 amplification and gene expression in breast cancer; association with proliferation and the non-basal subtypes, Breast Cancer Res. Treat. 180 (1) (2020) 73–86, https://doi.org/10.1007/s10549-020-05532-6.
[4] M. Cai, H. Li, R. Chen, X. Zhou, MRPL13 promotes tumor cell proliferation, migration and EMT process in breast cancer through the PI3K-AKT-mTOR pathway, Cancer Manag. Res. 13 (2021) 2009–2024, https://doi.org/10.2147/CMAR.S296038.
[5] S. Min, Y.K. Lee, J. Hong, et al., MRPS31 loss is a key driver of mitochondrial deregulation and hepatocellular carcinoma aggressiveness, Cell Death Dis. 12 (11) (2021) 1076, https://doi.org/10.1038/s41419-021-04370-8.
[6] K.O. Lam, W.W.L. Chan, T.H. So, D.L.W. Kwong, Systemic therapy for esophageal squamous cell carcinoma, Methods Mol. Biol. 2129 (2020) 321–333, https://doi.org/10.1007/978-1-0716-0377-2_24.
[7] B.Y. Wang, J.Y. Huang, H.C. Chen, et al., The comparison between adenocarcinoma and squamous cell carcinoma in lung cancer patients, J. Cancer Res. Clin. Oncol. 146 (1) (2020) 43–52, https://doi.org/10.1007/s00432-019-03079-8.
[8] Y. Ding, L. Zhang, L. Guo, et al., Comparative study on the mutational profile of adenocarcinoma and squamous cell carcinoma predominant histologic subtypes in Chinese non-small cell lung cancer patients, Thorac Cancer 11 (1) (2020) 103–112, https://doi.org/10.1111/1759-7714.13208.
[9] C. Wang, Q. Yu, T. Song, et al., The heterogeneous immune landscape between lung adenocarcinoma and squamous carcinoma revealed by single-cell RNA sequencing, Signal Transduct. Targeted Ther. 7 (1) (2022) 289, https://doi.org/10.1038/s41392-022-01130-8.
[10] Y. Tian, X. Zhai, W. Yan, H. Zhu, J. Yu, Clinical outcomes of immune checkpoint blockades and the underlying immune escape mechanisms in squamous and adenocarcinoma NSCLC, Cancer Med. 10 (1) (2021) 3–14, https://doi.org/10.1002/cam4.3590.
[11] L. Chen, M.F. Cao, X. Zhang, et al., The landscape of immune microenvironment in lung adenocarcinoma and squamous cell carcinoma based on PD-L1 expression and tumor-infiltrating lymphocytes, Cancer Med. 8 (17) (2019) 7207–7218, https://doi.org/10.1002/cam4.2580.
[12] S. Spranger, R. Bao, T.F. Gajewski, Melanoma-intrinsic beta-catenin signalling prevents anti-tumour immunity, Nature 523 (7559) (2015) 231–235, https://doi.org/10.1038/nature14404.
[13] M.A. Deken, J. Gadiot, E.S. Jordanova, et al., Targeting the MAPK and PI3K pathways in combination with PD1 blockade in melanoma, OncoImmunology 5 (12) (2016), e1238557, https://doi.org/10.1080/2162402X.2016.1238557.
[14] G. Abril-Rodriguez, D.Y. Torrejon, W. Liu, et al., PAK4 inhibition improves PD-1 blockade immunotherapy, Nat. Can. (Ott.) 1 (1) (2020) 46–58, https://doi.org/10.1038/s43018-019-0003-0.
[15] W. Ma, Y. Wang, R. Zhang, et al., Targeting PAK4 to reprogram the vascular microenvironment and improve CAR-T immunotherapy for glioblastoma, Nat. Can. (Ott.) 2 (1) (2021) 83–97, https://doi.org/10.1038/s43018-020-00147-8.
[16] W. Peng, J.Q. Chen, C. Liu, et al., Loss of PTEN promotes resistance to T cell-mediated immunotherapy, Cancer Discov. 6 (2) (2016) 202–216, https://doi.org/10.1158/2159-8290.CD-15-0283.
[17] T. Li, J. Fan, B. Wang, et al., TIMER: a web server for comprehensive analysis of tumor-infiltrating immune cells, Cancer Res. 77 (21) (2017) e108–e110, https://doi.org/10.1158/0008-5472.Can-17-0307.
[18] Y. Yu, Y. Sun, Z. Li, J. Li, D. Tian, Systematic analysis identifies XRCC4 as a potential immunological and prognostic biomarker associated with pan-cancer, BMC Bioinf. 24 (1) (2023) 44, https://doi.org/10.1186/s12859-023-05165-8.
[19] Z. Tang, B. Kang, C. Li, T. Chen, Z. Zhang, GEPIA2: an enhanced web server for large-scale expression profiling and interactive analysis, Nucleic Acids Res. 47 (W1) (2019) W556–w560, https://doi.org/10.1093/nar/gkz430.
[20] B. Ru, C.N. Wong, Y. Tong, et al., TISIDB: an integrated repository portal for tumor-immune system interactions, Bioinformatics 35 (20) (2019) 4200–4202, https://doi.org/10.1093/bioinformatics/btz210.
[21] J.C.T. Lim, J.P.S. Yeong, C.J. Lim, et al., An automated staining protocol for seven-colour immunofluorescence of human tissue sections for diagnostic and prognostic use, Pathology 50 (3) (2018) 333–341, https://doi.org/10.1016/j.pathol.2017.11.087.
[22] M. Surace, L. Rognoni, J. Rodriguez-Canales, K.E. Steele, Characterization of the immune microenvironment of NSCLC by multispectral analysis of multiplex immunofluorescence images, Methods Enzymol. 635 (2020) 33–50, https://doi.org/10.1016/bs.mie.2019.07.039.
[23] M. Emdadul Haque, D. Grasso, C. Miller, L.L. Spremulli, A. Saada, The effect of mutated mitochondrial ribosomal proteins S16 and S22 on the assembly of the small and large ribosomal subunits in human mitochondria, Mitochondrion 8 (3) (2008) 254–261, https://doi.org/10.1016/j.mito.2008.04.004.
[24] S. Gruschke, K. Grone, M. Heublein, et al., Proteins at the polypeptide tunnel exit of the yeast mitochondrial ribosome, J. Biol. Chem. 285 (25) (2010) 19022–19028, https://doi.org/10.1074/jbc.M110.113837.

[25] Z. Tao, H. Suo, L. Zhang, et al., MRPL13 is a prognostic cancer biomarker and correlates with immune infiltrates in breast cancer, OncoTargets Ther. 13 (2020) 12255–12268, https://doi.org/10.2147/OTT.S263998.
[26] K. Wang, L. Li, L. Fu, et al., Integrated bioinformatics analysis the function of RNA binding proteins (RBPs) and their prognostic value in breast cancer, Front. Pharmacol. 10 (2019) 140, https://doi.org/10.3389/fphar.2019.00140.
[27] H. Ye, N. Zhang, Identification of the upregulation of MRPL13 as a novel prognostic marker associated with overall survival time and immunotherapy response in breast cancer, Comput. Math. Methods Med. 2021 (2021), 1498924, https://doi.org/10.1155/2021/1498924.
[28] X. Zhou, C. Xiao, T. Han, et al., Prognostic biomarkers related to breast cancer recurrence identified based on Logit model analysis, World J. Surg. Oncol. 18 (1) (2020) 254, https://doi.org/10.1186/s12957-020-02026-z.
[29] X. Lin, L. Guo, X. Lin, Y. Wang, G. Zhang, Expression and prognosis analysis of mitochondrial ribosomal protein family in breast cancer, Sci. Rep. 12 (1) (2022), 10658, https://doi.org/10.1038/s41598-022-14724-7.
[30] Y. Liu, H. Sun, X. Li, et al., Identification of a three-RNA binding proteins (RBPs) signature predicting prognosis for breast cancer, Front. Oncol. 11 (2021), 663556, https://doi.org/10.3389/fonc.2021.663556.
[31] Y. Lan, J. Su, Y. Xue, et al., Analysing a novel RNA-binding-protein-related prognostic signature highly expressed in breast cancer, J Healthc Eng 2021 (2021), 9174055, https://doi.org/10.1155/2021/9174055.